21st Australasian Fluid Mechanics Conference
Adelaide, Australia
10-13 December 2018

Influence of Pressure Gradient on Plane Wake Evolution in a Constant Area Section

Chitrarth Lav, Richard D. Sandberg and Jimmy Philip

Department of Mechanical Engineering
University of Melbourne, Victoria 3010, Australia

Abstract

This study focusses on understanding the influence of streamwise pressure gradients acting in a constant area section on the spatial wake evolution. First, the impact of a constant area section in contrast to the usual variable area section is studied analytically for a simplified 2D inviscid flow. Second, high-fidelity data (DNS) is used to verify some of the conclusions of the above study. A flat plate normal to the flow at a Reynolds number of 2,000, based on the plate height and freestream velocity is considered as the test case for the high-fidelity calculations. Multiple pressure gradients are simulated to identify any global trends and compare with the existing experimental findings of variable area sections. The results indicate that the wake evolution in presence of a pressure gradient is dissimilar for constant and variable area sections.

Introduction

The study of turbulent wakes subjected to pressure gradients is as relevant today as it was when first examined by Hill [1] in the 1960s. Most experimental and numerical investigations have considered wake evolution where the pressure gradient is imposed by changing the area downstream, as encountered in diffusers or nozzles [1, 4, 6, 10]. However, in other applications, such as those found in the rotor-stator gap in multi-stage turbines and compressors, pressure gradients caused by the blade's potential field affect the wake evolution in a constant area section; and to the author's knowledge, this has received very little attention. Thus, the focus of the present study is on the effect of pressure gradients on wake evolution in a constant area section. The motivation for this study is illustrated in Figure 1, which shows the streamwise pressure gradient distribution for a low pressure turbine (LPT) cascade [7]. The area of interest is downstream of the blade trailing edge (TE), outlined in red.

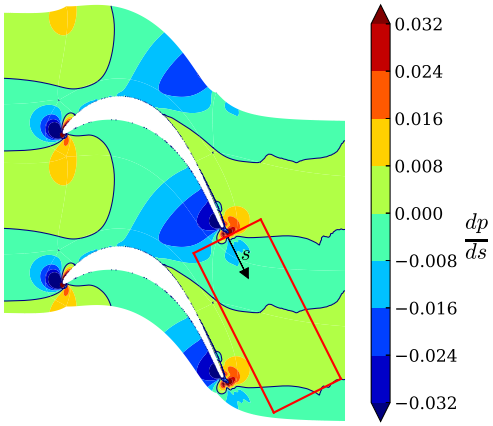

Figure 1: Streamwise pressure gradient for LPT stage at Re = 2,000, based on TE thickness and exit velocity. The domain of interest is outlined in red, and s is the local streamwise direction shown by the arrow.

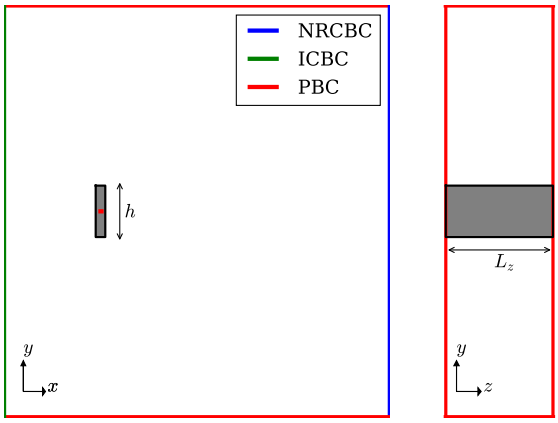

Figure 2: Schematic of canonical case with a constant area section. ICBC: Integrated Characteristic (inflow), NRCBC: Non-reflecting Characteristic (outflow), PBC: Periodic Boundary Conditions

Since the LPT case is a rather complex setup, owing to the upstream disturbances, this problem is studied canonically using a rectangular domain with a flat plate (of non-dimensional height $h = 1.0$ unit) normal to the flow as the wake generating body. The constant area section is modelled through periodicity in the y direction (see Figure 2). All variables have been non-dimensionalised with their corresponding scales evaluated at the domain inlet i.e. velocity scaled with U_o (uniform velocity of the domain inlet), density scaled with ρ_o (density of domain inlet), half-width, streamwise and cross-stream distances scaled with h. Pressure is normalised with the dynamic pressure, $0.5\rho_o U_o^2$. Other details about the domain are expanded upon later.

This paper is divided in three major parts: effect of area change, numerical setup and results. The first part analytically evaluates the differences between area change and constant area sections. The second part details the numerical setup for the high-fidelity simulations, and the final part presents the results of the simulations.

Effect of Area Change

In this section, the difference between pressure gradients acting in a constant area (CA) section is compared with a variable area (VA) section analytically. The sections are shown in Figure 3 where, to simplify the problem, two-dimensional inviscid flow is assumed, flowing from left to right. The boundaries in the y direction for CA are defined as periodic while the boundaries for VA are defined as slip walls. Assuming the flow states (density, velocity and pressure) at the inlet for the two sections is the same and that the velocities at the outlet are the same between the two sections, a control volume analysis of the sections may be performed to relate the pressure gradients in the two sections. The continuity equation for CA and VA, respectively, is given

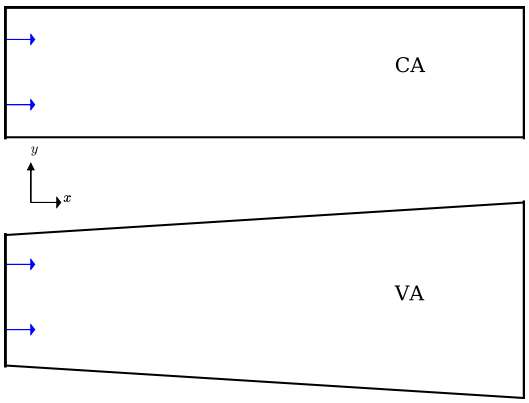

Figure 3: Constant area section (top) and variable area section (bottom) schematic. Blue arrows represent mean flow direction

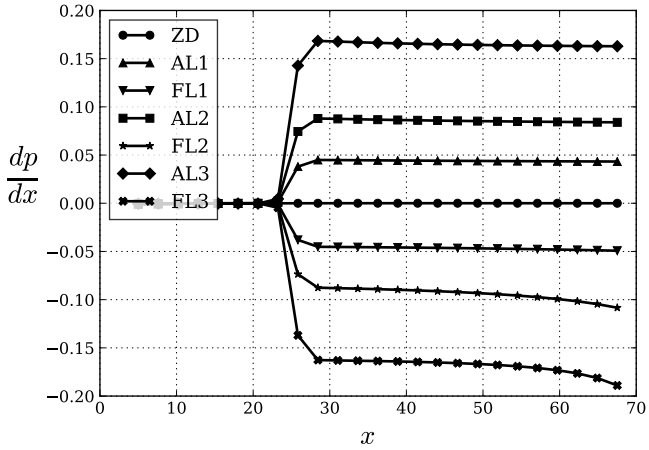

Figure 4: Pressure gradients in the freestream for the cases considered. The legends are defined in Table 1.

by:

$$\rho_i u_i = \rho_{o,CA} u_o, \quad (1)$$

$$\rho_i u_i A_i = \rho_{o,VA} u_o A_o. \quad (2)$$

The subscipts i, o refer to the inlet and outlet locations, while A refers to the cross-section area. Using the earlier assumptions, the density at the outlet for the two cases can be related by

$$\rho_{o,CA} = \rho_{o,VA} \frac{A_o}{A_i}. \quad (3)$$

Thus, for an adverse gradient ($A_o > A_i$), the value of density in CA is higher than the value in VA and vice versa for a favorable gradient. Next, applying the control volume momentum conservation for each section can be written as:

$$\rho_{o,CA} u_o^2 - \rho_i u_i^2 = p_i - p_{o,CA}, \quad (4)$$

$$\rho_{o,VA} A_o u_o^2 - \rho_i A_i u_i^2 = p_i A_i - p_{o,VA} A_o. \quad (5)$$

Using the same assumptions as before, and dividing the above equations by the length of the sections (L), the pressure gradients for the two sections can be related by:

$$\left(\frac{p_{o,CA} - p_i}{L}\right) = \left(\frac{p_{o,VA} - p_i}{L}\right)\frac{A_o}{A_i} + \frac{p_i}{L}\left(\frac{A_o}{A_i} - 1\right),$$

$$\left.\frac{\Delta p}{\Delta x}\right|_{CA} = \left.\frac{\Delta p}{\Delta x}\right|_{VA} \frac{A_o}{A_i} + \frac{p_i}{L}\left(\frac{A_o}{A_i} - 1\right). \quad (6)$$

It can be seen that to maintain the same values of velocity, the values of pressure gradients between the two sections are different. For both favorable ($p_o < p_i$) and adverse ($p_o > p_i$) gradients, the CA section requires a larger magnitude of the pressure gradient compared with the VA section, to maintain the same velocites. The major conclusions with this investigation are twofold: pressure gradient affects the density for the CA section and higher pressure gradients are needed with CA sections to produce the same outlet velocities as in VA sections, given the same inlet conditions.

Numerical Setup

To consider plane wake evolution in constant area sections, a numerical investigation is conducted using a high-fidelity code (HiPSTAR), which is an in-house structured compressible Navier-Stokes solver. The code is finite difference based, using a standard fourth-order accurate stencil in space and a fourth-order accurate Runge-Kutta scheme in time [7]. The code can undertake Direct Numerical and Large Eddy Simulations. All cases presented here were run as LESs with some cases also run as DNSs to serve as anchor points. The schematic of the domain, along with the boundary conditions, is shown in Figure 2. Due to the compressible nature of the code, characteristic boundary conditions [2, 3] are employed, to prevent spurious reflection from the inflow/outflow boundaries. Thus, integrated characteristic (ICBC) for the inflow and non-reflecting characteristic (NRCBC) for the outflow are used. The outflow boundary is also combined with a zonal boundary condition, which acts as sponge to damp out any reflections back into the domain [8]. The spanwise direction (z) is solved in Fourier space to reduce computational effort, and as such the spanwise boundaries are periodic. Grid and domain size convergence tests were conducted on the zero pressure gradient (ZPG) configuration for the DNS to ensure the smallest length scales were being resolved. The final domain chosen for the investigation extends from -15 to 85 units in the x direction, -20 to 20 units in the y direction and the spanwise extent is 8 units. The flat plate was placed at the origin of this domain, with a height and thickness of 1 and 0.1 units respectively. The grid around the flat plate was not body-fitted, but represented with the Boundary Data Immersion Method (BDIM) [9], whereby a smoothing region is used to demarcate the boundaries of the flat plate. The flow variables are ramped down to zero from outside of the smoothing region (the fluid domain) to the inside of the smoothing region (the flat plate domain). The domain dimensions were non-dimensionalised with the plate height. All simulations were conducted at a Re = 2,000, based on the plate height and freestream velocity. The resultant grid contained 1056×396 points in the $x-y$ plane and 64 Fourier modes in the spanwise direction. Finding the optimal grid for the LES cases involved coarsening the DNS grid until the results of the LES were significantly different. This resulted in the optimal LES grid containing 672×290 points in the $x-y$ plane with 64 Fourier modes. Four LES models were also subjected to tests to identify the most suitable choice, with the Wall-Adapting Local Eddy Viscosity (WALE) model [5] acheiving the best agreement with the DNS for the zero pressure gradient case. The pressure gradient simulations were performed by adding a streamwise ramp based forcing term to the u momentum and energy equations. A smooth ramp was considered to prevent a sudden jump in the pressure gradient and was applied 25 units downstream of the flat plate. This setup

was choosen as it provided the same upstream condition for all cases so that the different pressure gradient cases can be compared. The streamwise pressure gradient evolution for the cases considered in the next section is shown in Figure 4, where the legends are defined in Table 1.

Results

In this section, multiple pressure gradient magnitude scenarios are considered, with both favourable (FPG) and adverse gradients (APG). Table 1 lists the cases considered for this investigation along with the legends used for various plots.

Pressure Gradient Cases		
Case Legend	Simulation	Pressure Gradient
ZD	DNS	+0.0
ZL	LES	+0.0
AL1	LES	+0.04
AL2	LES	+0.08
AL3	LES	+0.16
AD3	DNS	+0.16
FL1	LES	-0.04
FL2	LES	-0.08
FL3	LES	-0.16
FD3	DNS	-0.16

Table 1: Cases considered for the investigation. 3 DNS studies serve as anchor points for the LES results

Initial simulations were performed with magnitudes of the gradients matching the experiments of Liu *et al* [4], who used adjustable walls to mimic a variable area section. It was observed that the results did not deviate significantly from the ZPG solution. Therefore, higher magnitudes were considered, as given in the table above. This finding is in agreement with the analytical conclusion between the CA and VA sections. Figure 5 shows a side profile of the instantaneous Q-criterion ($Q = 0.5[|\Omega|^2 - |S|^2]$, where $|\Omega|, |S|$ are mean rotation and strain rate respectively). The isosurfaces are coloured by the spanwise vorticity for the extreme cases AL3 and FL3 for visual comparison. The FL3 field shows dominance of large elongated structures as compared with the AL3 case, which shows a mix of different sized structures which persist until much further downstream.

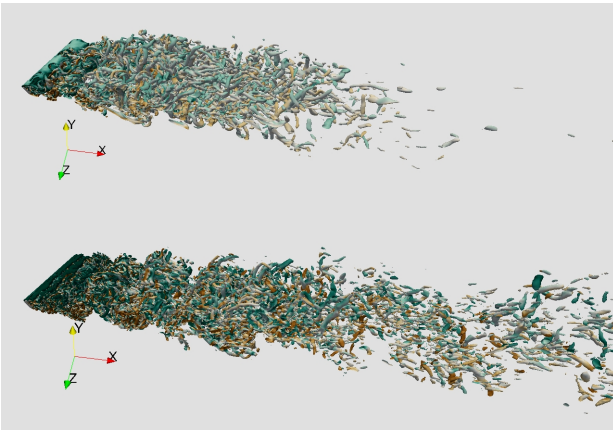

Figure 5: Q-criterion isosurfaces at normalised value of 0.001, coloured by the spanwise vorticity; (top) FL3 (bottom) AL3

Figure 6 shows the u and ρ profiles for the different cases at $x = 50.0$. This figure shows that an increase in the velocity is compensated by a reduction in density and vice versa, to conserve the total flux. A control volume analysis did indeed show that the flux was being conserved, for all the cases.

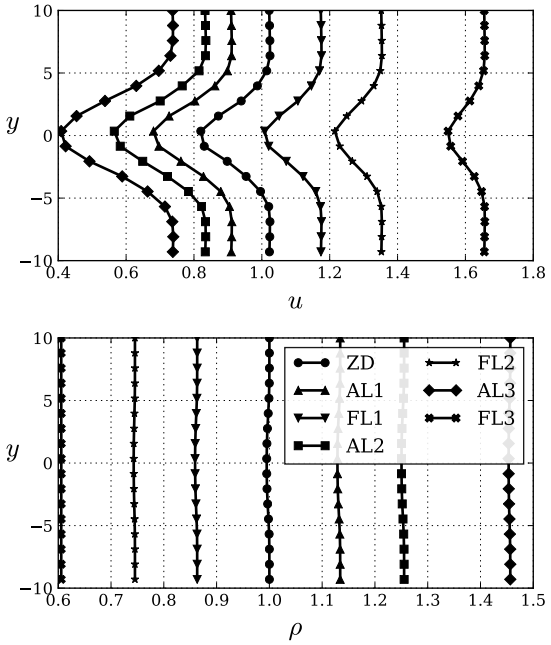

Figure 6: Profiles of u and ρ at $x = 50.0$.

The effect of the pressure gradients can also be studied through the two wake parameters: maximum wake velocity deficit (U_d) and wake half-width (δ). U_d is defined as the difference between the freestream velocity and the minimum velocity while δ is defined as the distance from the wake centerline to the point where the local deficit is half of the maximum deficit, i.e. $0.5U_d$. Figure 7 shows the streamwise evolution of U_d and δ. Key observations for the different cases are:

- For the ZPG case, the evolution follows the usual scalings for U_d ($\sim x^{-0.5}$) and δ ($\sim x^{0.5}$) respectively, which has been observed experimentally for far wakes in a ZPG environment [4, 11].
- Positive pressure gradients show a larger growth in δ compared with the ZPG. The APG considered by Liu *et al* [4] also showed an increment, though the fitted function there was an exponential, which is not observed here.
- The δ for all FPG cases closely follows the ZPG with a scaling of 0.5. This is quite different comparing with the VA experiments [4], which showed a smaller rate of growth in δ values for the two FPG cases. However, higher magnitudes of FPG need to be run to verify if the scaling observed here changes.
- The deficit velocities exhibit similar behaviour as expected from VA sections for both pressure gradient regimes. High values of APGs suggest a recovery of deficit back to pre-application of pressure gradients while high FPGs shows an almost exponential decline in the deficit.

Conclusions

In this study, the effect of pressure gradients on the streamwise wake evolution in a constant area section was investigated. The

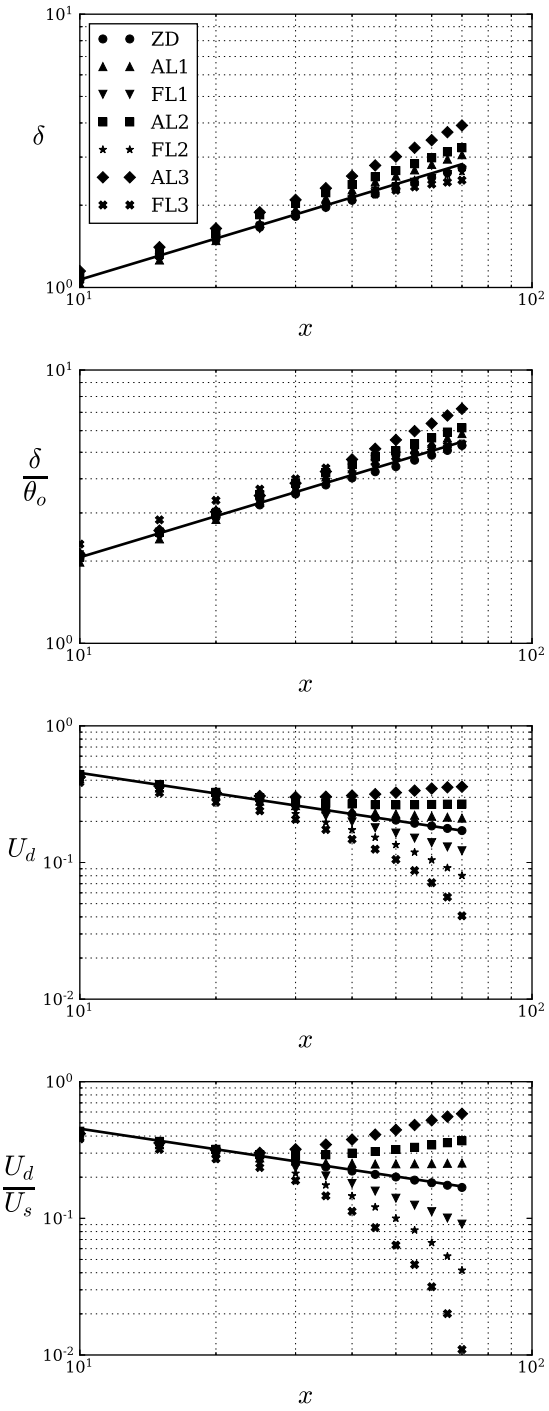

Figure 7: Wake parameters U_d, δ evolution in x. U_s is the local freestream velocity and θ_o is momentum thickness upstream of ramping location at $x = 20.0$

impact of a constant area section was first analysed using a simplified model where compressibility was found to have a more significant contribution for the constant area sections. It was also observed that different magnitudes of pressure gradients are required to obtain the same evolution in the streamwise velocity for constant and variable area sections. The second part of the study involved conducting high-fidelity simulations of a wake, subjected to different pressure gradients. It was observed that higher magnitudes were necessary to demonstrate the behaviour as seen in the variable area experiments, which matches the conclusion from the theoretical analysis. The results were however true only for the velocity deficit while the wake half-widths exhibited entirely different evolution compared with the VA experiments. These sets of results indicate that the effect of the pressure gradient in a constant area section does not have trivial solutions and requires a much more detailed analysis, both analytically and numerically, to explain the trends seen here.

Acknowledgements

This work was supported by resources provided by the Pawsey Supercomputing Centre with funding from the Australian Government and the Government of Western Australia. This work also acknowledges financial support from the Australian Research Council.

References

[1] Hill, P. G., Schaub, U. W. and Sendo, Y., Turbulent wakes in pressure gradients, *ASME J. Appl. Mech.*, **30**, 1963, 518–524.

[2] Kim, J. W. and Lee, D. J., Generalized Characteristic Boundary Conditions for Computational Aeroacoustics, Part 2, *AIAA J.*, **42**, 2004, 47–57.

[3] Kim, J. W. and Sandberg, R. D., Efficient parallel computing with a compact finite difference scheme, *Comput. Fluids*, **58**, 2012, 70–87.

[4] Liu, X., Thomas, F. O. and Nelson, R. C., An experimental investigation of the planar turbulent wake in constant pressure gradient, *Phys. Fluids*, **14**, 2002, 2817–2838.

[5] Nicoud, F. and Ducros, F., Subgrid-Scale Stress Modelling Based on the Square of the Velocity Gradient Tensor, *Flow, Turbul. Combust.*, **62**, 1999, 183–200.

[6] Rogers, M. M., The evolution of strained turbulent plane wakes, *J. Fluid Mech.*, **463**, 2002, 53–120.

[7] Sandberg, R. D., Michelassi, V., Pichler, R., Chen, L. and Johnstone, R., Compressible direct numerical simulation of low-pressure turbines: part I - methodology, *J. Turbomach.*, **137**, 2015, 51011.

[8] Sandberg, R. D. and Sandham, N. D., Nonreflecting Zonal Characteristic Boundary Condition for Direct Numerical Simulation of Aerodynamic Sound, *AIAA J.*, **44**, 2006, 402–405.

[9] Schlanderer, S. C., Weymouth, G. D. and Sandberg, R. D., The boundary data immersion method for compressible flows with application to aeroacoustics, *J. Comput. Phys.*, **333**, 2016, 440–461.

[10] Tummers, M. J., Hanjalić, K., Passchier, D. M. and Henkes, R. A. W. M., Computations of a turbulent wake in a strong adverse pressure gradient, *Int. J. Heat Fluid Flow*, **28**, 2007, 418–428.

[11] Wygnanski, I., Champagne, F. and Marasli, B., On the large-scale structures in two-dimensional, small-deficit, turbulent wakes, *J. Fluid Mech.*, **168**, 1986, 31–71.